Single-Wall Nanotube Models

DOI: 10.1002/ange.201400719

Properties of Sizeable [*n*]Cycloparaphenylenes as Molecular Models of Single-Wall Carbon Nanotubes Elucidated by Raman Spectroscopy: Structural and Electron-Transfer Responses under Mechanical Stress**

Miriam Peña Alvarez, Paula Mayorga Burrezo, Miklos Kertesz, Takahiro Iwamoto, Shigeru Yamago, Jianlong Xia, Ramesh Jasti, Juan T. López Navarrete, Mercedes Taravillo, Valentín G. Baonza,* and Juan Casado**

Abstract: *[n]Cycloparaphenylenes behave as molecular templates of "perfectly chemically defined" single-wall carbon nanotubes. These [n]CPP molecules have electronic, mechanical, and chemical properties in size correspondence with their giant congeners. Under mechanical stress, they form charge-transfer salts, or complexes with fullerene, by one-electron concave–convex electron transfer.*

A given [*n*]cycloparaphenylene ([*n*]CPP) can be considered as the shortest length cylindrical version of (*n*,*n*) armchair single-wall carbon nanotubes (SWCNTs; Figure 1). The unique tubular shape of SWCNTs is key for their outstanding optical, electronic, and mechanical properties, which are the basis of their applications as unique nanomaterials.[1,2] However, a full understanding of the molecular foundation of these outstanding characteristics is still incomplete, which is due, among other factors, to difficulties in the chemical definition of SWCNTs, a drawback which is intimately related to current syntheses and the absence of orthodox methods for their bottom-up chemical preparation.[2] In this regard,

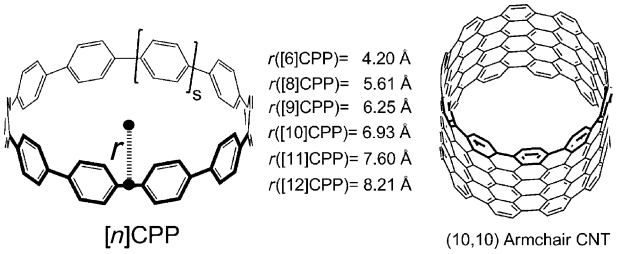

Figure 1. Chemical structure of [*n*]CPP, $n = 6$–12, with $n = 10 - s$ and $s = 4, 3, 2, 1, 0, -1$, and -2. r = [*n*]CPP radius. Radii are taken from references [3–9].

[*n*]CPPs are perfectly-defined hydrocarbon compounds envisioned as the cyclization of long linear oligo[*n*]paraphenylenes,[3–9] and have been already prepared by well-established organic synthetic reactions.[3–9] Very recently, significant progress has been made with the demonstration of the preparation of SWCNTs using [*n*]cycloparaphenylene molecules as templates.[2a,10]

In our interest of exploring possible mechanical, chemical and spectroscopic analogies between [*n*]CPPs and SWCNTs, we here study [*n*]CPPs in an oligomeric approach to SWCNTs. Furthermore, the study of the [*n*]CPPs might provide relevant insights about the exclusive properties imparted by their unique belt-shape or nanohoop structure and relate them to known properties of SWCNTs. Furthermore, [*n*]CPPs are significant on their own right given their salient optoelectronic and structural properties,[3–9,11] and their host–guest ability to form supramolecular assemblies[7,12] (van der Waals nanotubes). The sizeable radius of the [*n*]CPPs together with their bendable peripheral cyclic π-electron delocalization provides us with an excellent opportunity to study their electronic, structural, and mechanical properties as a function of the precise chemical structure.

Raman spectroscopy has been established as the most suitable method to probe the molecular and electronic structure of sp^2-carbon nanostructures[13] and to establish structure–property relationships in SWCNTs allowing the formulation of structural–spectroscopic correlations. In particular, the frequency of the radial breathing mode (RBM), ν(RBM), is used to estimate the diameter distribution in SWCNTs based on its linear trend with the inverse of the tube diameter d.[14] Herein, we use Raman spectroscopy to probe the molecular level changes in the electronic structure of [*n*]CPPs as a function of their sizes/diameters (Figure 1) from

[*] P. M. Burrezo, Prof. J. T. L. Navarrete, Prof. J. Casado
Department of Physical Chemistry, University of Málaga
CEI Andalucía Tech, Campus de Teatinos s/n, 29071-Málaga (Spain)
E-mail: casado@uma.es
M. P. Alvarez, Prof. M. Taravillo, Prof. V. G. Baonza
MALTA-Consolider Team, Department of Physical Chemistry
Chemistry Faculty, University Complutense of Madrid
28040 Madrid (Spain)
Dr. T. Iwamoto, Prof. S. Yamago
Institute for Chemical Research, Kyoto University
Uji 611-0011 (Japan)
Prof. M. Kertesz
Department of Chemistry and Institute of Soft Matter, Georgetown University
37th and O Streets, NW, Washington, D.C. 20057-1227 (USA)
J. Xia, Prof. R. Jasti
Department of Chemistry and Division of Materials Science & Engineering and Center for Nanoscience & Nanotechnology, Boston University
24 Cummington St., Boston, MA 02215 (USA)

[**] Financial support from MINECO of Spain (CTQ2012-33733), CTQ2012-38599-C02-02, CSD2007-00045, Junta de Andalucía (Project P09-FQM-4708), and Comunidad de Madrid (S2009/PPQ-1551) are acknowledged. M.P.A. is grateful to the Spanish MEC for an FPU grant.

Supporting information for this article is available on the WWW under http://dx.doi.org/10.1002/anie.201400719.

[6]CPP to [12]CPP, aiming to get new structural and chemical insights within the context of molecular strain, peripheral or cyclic π-electron delocalization, mechanical flexibility, and host–guest properties. The latter aspect deserves special mention, as we have realized a novel full charge-transfer host–guest complex between [10]CPP and C_{60} promoted under high pressure, which contrasts with that well-known supramolecular complex solely formed by π···π van der Waals concave–convex interactions.[7] The interpretation of these phenomena is guided by quantum-chemical calculations that included full geometry optimizations and frequency and intensity (Raman and IR) calculations at the B3LYP/6-31G* level. Frequencies were scaled with the uniform scaling factor of 0.97.

Figure 2 shows the 785 nm excitation Raman spectra for the seven [*n*]CPP compounds. The low wavenumber regions of [10]CPP and [12]CPP are clearly dominated by single bands at 286 and 242 cm^{-1}, respectively, that would belong in principle to RBM radial-like modes. To check this hypothesis,

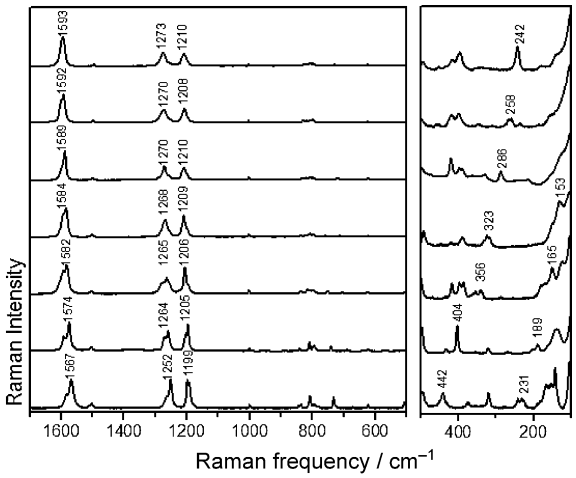

Figure 2. 785 nm Raman spectra of the compounds in solid state at room temperature. From bottom to top: [6]CPP to [12]CPP.

we have carried out quantum chemical calculations of the vibrational Raman spectra for the most stable conformers of the [*n*]CPPs (Supporting Information, Section S1). We noticed that the two bands above are predicted at 274 and 233 cm^{-1} in [10]CPP and [12]CPP (Supporting Information, Figures S2.1, S3.1, and S.4.1 and Tables S2.1, S3.1, and S4.1); however, correspond to E_{2g} or E_2 symmetry modes, thus not representing true RBM modes, which are totally symmetric modes. In the shorter [*n*]CPPs, the low frequency region is much more complex, and only with the help of the predicted theoretical spectra we are able to assign the E_{2g} or E_2 modes in the Raman spectra at 258, 323, 356, 404, and 442 cm^{-1} in [11]-, [9]-, [8]-, [7]-, and [6]CPP, respectively. Interestingly, as the radii of these molecules are known (Figure 1), we found a clear linear dependence of their frequencies on $1/d$ (Scheme 1 a), which is a unique property of the RBM modes in SWCNTs, so we suggest to label them as pseudo-RBM modes. The calculated spectra also permit to assign the true totally symmetric RBM modes to those bands at 153, 165,

a $\omega_{p-RBM}\,(cm^{-1}) = (8\pm3) + \frac{(375\pm3)}{d(nm)}$

b $\omega_{RBM}\,(cm^{-1}) = (-3\pm6) + \frac{(197\pm5)}{d(nm)}$

Strain Energy(kJ/mol) $= (14\pm7) + (0.74\pm0.04) * \omega_{p-RBM}\,(cm^{-1}) + (3.2\pm0.6)\cdot10^{-4} * \omega_{p-RBM}{}^{2}\,(cm^{-2})$

Scheme 1. $\nu(cm^{-1})$-$(1/d)$ fits for the pseudo-RBM (a), and RBM (b) in [*n*]CPPs. Strain energy as a function of the pseudo-RBM Raman frequency. See the Supporting Information, Figure S4.2 for details.

189, and 231 cm^{-1} in [9]-, [8]-, [7]-, and [6]CPP, respectively. Interestingly, fitting the frequencies of these modes against $(1/d)$, we obtain a very similar slope (197 nm cm^{-1}) to that typically found in SWCNTs (227 nm cm^{-1}; Scheme 1).

The nearly cylindrical shape of the [*n*]CPPs implies a strain component on its formation energy, which accounts for the positive work owing to rolling and cycling a linear oligophenylene of the same size.[15] We have represented in Figure 3 the variation of the strain energy and the pseudo-RBM frequency with the number of rings. As both energetic

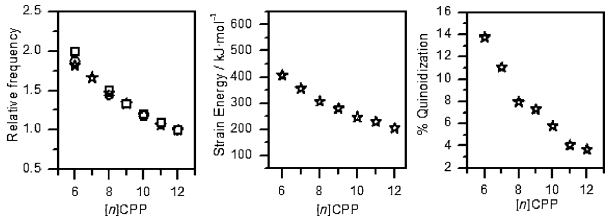

Figure 3. Left: Relative frequency (ν ([*n*]CPP pseudo-RBM modes)/ ν ([12]CPP pseudo-RBM mode) experimental (stars) and theoretical (circles); and ($\nu((n,n)$ SWCNT-RBM modes)/ν((12,12) SWCNT-RBM modes) with square symbols) as a function of *n*, SWCNTs data.[16] Middle: Variation of the strain energy[15] of the [*n*]CPP as a function of *n*. Right: Variation of the per-ring quinonoid character as a function of *n* (see the Supporting Information, Section S6 for details).

and spectroscopic parameters display the same trend, the pseudo-RBM frequencies in the [*n*]CPPs (and the RBM frequencies in SWCNTs) can be considered as experimental observables of the strain energy according to the expression given in Scheme 1. In Figure 3, taking [12]CPP as a reference, we compare both the [*n*]CPPs pseudo-RBM frequencies and the corresponding RBM ones of (*n*,*n*) armchair SWCNTs divided by that of the [12]CPP (E_2) and (12, 12) SWCNTs (A_{1g}), respectively. We observe a good match between these ratios, suggesting that [*n*]CPPs again mimic the relevant structural properties of SWCNTs, despite their different chemical constitution.

In the 1560–1600 cm^{-1} range the most intense Raman bands appear at 1567 cm^{-1} in [6]CPP, 1574 cm^{-1} in [7]CPP, 1582 cm^{-1} in [8]CPP, 1584 cm^{-1} in [9]CPP, 1589 cm^{-1} in [10]CPP, 1592 cm^{-1} in [11]CPP, and 1593 cm^{-1} in [12]CPP. These bands originate from totally symmetric vibrations arising from collective CC stretching modes of the benzenoid rings along the transversal tube axis direction (Supporting Information, Figures S2.1 and S3.1 and Tables S2.1 and S3.1). All of the [*n*]CPPs show sub-bands at higher frequencies (1600–1610 cm^{-1}) owing to localized transversal modes, which reside on alternant rings. The transversal character of both

bands resemble that of G^+ band in armchair SWCNTs.[16,17] However, no G^- modes are recognized owing to the absence of a well-defined longitudinal direction in the [*n*]CPPs (Supporting Information, Tables S2.1 and S3.1).[17] These modes derive from the 8a mode in benzene, which allows us to analyze the benzoquinonoid nature of such molecular structures. It is well known that 8a mode frequencies around 1600 cm^{-1} are characteristic of benzo-aromatic moieties, while down-shifted frequencies are typical of benzoquinonoid moieties.[18] Such a correlation between Raman frequencies and aromatic-quinonoid character is further corroborated by the oxidation of [10]CPP to its radical cation ([10]CPP$^{\bullet+}$; Figure 5), which unequivocally provokes ring quinoidization, and shows the main Raman band at 1569 cm^{-1}. The detection of the G bands between 1565–80 cm^{-1} in the shorter [*n*]CPP indicates that their rings are partially quinoidized, or that benzene aromaticity is partially broken due to two main effects: 1) The inter-ring connecting carbons become pyramidalized ($sp^2 \rightarrow sp^3$ evolution) and 2) the rings are slightly bent to accommodate the macrocyclic curvature and to mitigate ring strain. The Raman band at 1567 cm^{-1} indicates a benzoquinonoid structure and strong cycle strain in [6]CPP, while that at 1595 cm^{-1} in [12]CPP reveals a slightly curved macrocycle with a ring aromatic character similar to that of linear oligoparaphenylenes (Supporting Information, Figure S5.1 and Table S5.1). The behavior of these bands has been further investigated as a function of the temperature and irradiation time, allowing interesting conformational properties of the [*n*]CPPs to be deduced (Supporting Information, Section S8).

The force field of a given molecule is the true connection between its vibrational observables (frequencies) and the electron density. A force constant analysis of the 1600 cm^{-1} Raman modes allows us to quantify a degree of quinoidization close to 14% per ring for the smallest [6]CPP (Figure 3; Supporting Information, Section S6). This indicates that quinoidization and $sp^2 \rightarrow sp^3$ re-hybridization owing to the curvature take place only in a moderate degree, which is sufficient to maintain the prevalent aromatic character of the rings as a condition to preserve chemical stability, even in the more strained member of the series [6]CPP. This distinctive partial quinonoid character might provoke an incipient activation for cycloaddition reactions, which would support the demonstration that SWCNTs grow by vertical condensation of [*n*]CPPs.[2]

Analyzing the bands appearing around 1190–1220 cm^{-1}, it is seen that they mainly emerge from in plane CH bending modes, β(CH), and those around 1260–1270 cm^{-1}, corresponding to ring breathing modes, ν(CC) (Supporting Information, Figure S7.1). The relative Raman intensity ratio, $I_{\nu(C\text{-}C)}/I_{\beta(CH)}$, in linear oligophenylenes has been related to the π-conjugation domain size as a function of the torsional angle (θ) between neighboring rings (that is, a larger ratio means higher torsional angle or smaller conjugation).[19] We have obtained $I_{\nu(C\text{-}C)}/I_{\beta(CH)}$ for each [*n*]CPP (Supporting Information, Figure S7.2) and noticed that it progressively increases with increasing the [*n*]CPP size. This might reveal smaller conjugation in the largest [12]CPP, thus confirming that in the larger [*n*]CPPs the behavior is closer to linear oligoparaphenylenes: thus, [12]CPP can be viewed as a collection of short linear oligophenylenes cyclically embedded to form a macrocycle. In this regard, large [*n*]CPPs behave as nearly equivalent to linear oligoparaphenylenes, which is in agreement with: 1) the almost full aromatic character of the rings in these relatively long compounds; and 2) the exponential variation of the ring strain with size, with a strong attenuation effect starting in [11]-[12]CPP.

Table 1 shows selected data from the optimized theoretical geometries. The inter-ring CC bonds are rather large for [6]CPP, revealing an inefficient orbital overlap between the $2p_z$ orbitals of adjacent benzenes. The rings disclose a typical quinoidal character ($r_1 < r_2$) that decreases with increasing *n*.

Table 1: B3LYP/6-31G* optimized geometries of the [*n*]CPP.[a]

[*n*]CPP	r(CC)$_{interring}$	r_1(CC)$_{ring}$	r_2(CC)$_{ring}$	θ	γ	θ[b]
6	1.490	1.393	1.410	27.1	150	36.0
8	1.487	1.391	1.407	30.7	157	–
10	1.485	1.392	1.407	32.8	162	–
12	1.484	1.390	1.406	33.5	165	35.9

[a] See the Supporting Information, Section S1 for the definition of the bond distances [Å] and angles [°]. [b] [*n*]LPP.

The θ inter-ring torsional angle increases with *n*, approaching those predicted for the linear parents. The γ angle (180° in [*n*]LPP) reveals that the curvature of the macrocycle is attained by forcing it from 180° what further interferes the coupling between vicinal $2p_z$ orbitals. This suggests that cyclic conjugation in the [*n*]CPPs has a different nature than standard linear conjugation, which is always driven by a maximal inter-ring p_z orbital overlap.

Internal strain can be modulated by application of external stresses or pressures, and such experiments have revealed key information about the structural and mechanical properties of SWCNTs.[20] We have therefore performed series of pressure-dependent Raman experiments using an anvil cell device[21] on the largest and smallest members, [6]CPP to [12]CPP; maximum pressures around 8–10 GPa were achieved. Figure 4 compares the Raman spectra measured at ambient conditions, high pressure, and after pressure

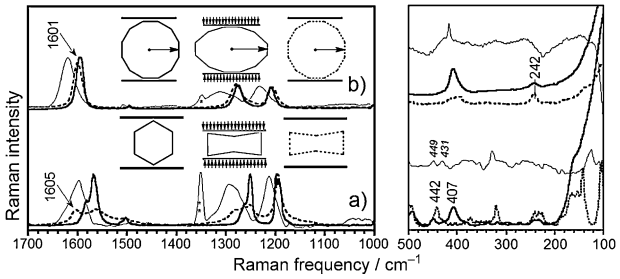

Figure 4. 785 nm Raman spectra of: a) [6]CPP and b) [12]CPP, before (solid line), with an applied pressure around 6 GPa (gray line) and after the pressure release (dotted line). Bands with asterisks correspond to the diamond used as pressure sensor. Inserted schemes represent (from left to right) the molecular models before applied pressure, with applied pressure, and after release.

release. In [12]CPP, pressure does not seem to cause any irreversible change, in clear contrast to that observed in [6]CPP, where significant frequency and spectral changes are found: the pseudo-RBM mode of [6]CPP shifts to lower values, and the 1600 cm^{-1} region is completely modified. The first observation suggests ovalization of the cycle (flattening) and formation of two pseudo-linear segments, more aromatic, which would be responsible of the bands at 1605 cm^{-1}. Such irreversibility in [6]CPP reveals that the cyclic shape collapses below 8 GPa and remains quenched in a sandwiched-like structure when the pressure is released to ambient conditions (see insert in Figure 4), a phenomenon already found in SWCNTs.[22,23] Similar pressure experiments are presented in the Supporting Information, Figure S9 for the [*n*]CPP molecules; changes before and after the pressure cycle are progressively smaller as the size increases, presumably because less strained molecules would require higher pressures to undergo an equivalent permanent deformation.

We have also conducted two challenging experiments under pressure. First, we used a 1:1 [6]CPP and [12]CPP mixtures aiming to encapsulate [6]CPP into [12]CPP just to emulate a ultrashort double walled CNT (DWCNT).[24a] The Raman spectra of the mixtures before and after the pressure cycle are displayed in the Supporting Information, Figure S10.1. Very small changes are observed in the Raman spectrum, thus indicating that pressure could promote encapsulation of [6]CPP into the internal cavity of [12]CPP, and thus preventing [6]CPP to collapse. This observation is in good agreement with previous results observed in DWCNTs, where the outer tube acts as pressure protector of the inner tube.[24]

The success of the [6]CPP encapsulation into [12]CPP under pressure, together with the fact that some [*n*]CPPs can also accommodate C_{60}-fullerene into their internal cavities, led us to explore the properties of [*n*]CPPs + C_{60} complexes, which is also in clear analogy with the "SWCNT + C_{60} peapods".[25,26] It is π–π interactions that are responsible for the assembly of some [*n*]CPPs with C_{60}, giving rise to the formation in solution of 1:1 stoichiometric supramolecular complexes driven by a surprisingly high *exo*-thermicity.[7] In particular, concave–convex π–π interactions are strongly promoted in these complexes owing to the natural curvature adjustment between the [*n*]CPP host and the C_{60} guest. We prepared 1:1 powdered mixtures of [10]CPP and C_{60} and applied pressures up to 6 GPa, which are well below the 22 GPa limit of chemical stability found for C_{60}.[27] Figure 5 displays the Raman spectra of the mixture recovered at ambient conditions after a pressure cycle. In the spectral range around 1460–1470 cm^{-1} we observe the two strongest Raman bands, one at the same frequency as pristine C_{60}, and another one at 1463 cm^{-1}. In the [10]CPP region at 1570–1600 cm^{-1} we observe a new band at 1569 cm^{-1} while the band at 1589 cm^{-1} disappears. Interestingly, the changes of these Raman bands in the [10]CPP@C_{60} complex formed in solution are very small, in accordance with π–π interactions that are unable to produce appreciable changes in the electronic structure of the individual components (supramolecular effect). Our observations in the experiment with pressure substantially differ from that described for the [10]CPP@C_{60} solution complex; as seen in Figure 5, pressure promotes the appearance of new Raman bands that correlate perfectly with those of the C_{60} radical anion ($C_{60}^{\bullet-}$)[27] and the [10]CPP radical cation ([10]CPP$^{\bullet+}$).

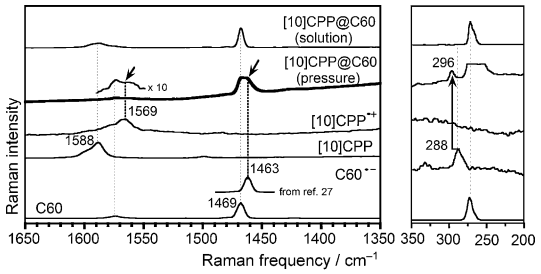

Figure 5. 785 nm Raman spectra of 1:1 $CHCl_3$ solution mixtures of [10]CPP and C_{60} and in solid state after the application of a 6 GPa pressure. The spectra of the neutral C_{60} and [10]CPP together with those of the C_{60} anion and of CPP radical cation are also shown.

The straightforward interpretation is that the application of pressure produces the releasing of one electron from the donor [10]CPP to the acceptor C_{60} yielding a charge-transfer charge-separated complex, or a [10]CPP$^{\bullet+}$@$C_{60}^{\bullet-}$ salt. We can reasonably assume that, as already demonstrated herein, pressure might induce flattening of the [10]CPP that approaches the electron-donor surface to the acceptor one to a distance feasible for the electron transfer, which is a situation that is unlikely to occur in solution. This electron-transfer reaction is a good example of the chemical reactivity in the electronic polarized cavity of [*n*]CPP provided that a suitable sandwiched transition state is formed.

We have also analyzed the frequency of the pseudo-RBM in the [10]CPP$^{\bullet+}$@$C_{60}^{\bullet-}$ complex which upshifts by 8 cm^{-1} (296 cm^{-1}). According to the (1/*d*) frequency dependence, this shift indicates a slight reduction of the [10]CPP size in the complex, or that the [10]CPP$^{\bullet+}$ is "compressed" owing to the loss of one electron and quinoidization of the structure with the concomitant decrease of the radius (the pseudo-RBM mode in [10]CPP$^{\bullet+}$ alone was undetected). The C_{60} band at 270 cm^{-1} scarcely shifts in the complex, in agreement with the barely observable displacement of just +1 cm^{-1} in K_3C_{60} ($C_{60}^{\bullet3-}$).[27]

Finally, similar complexation experiments of C_{60} under pressure have been carried out with [9]CPP and [11]CPP (Supporting Information, Figure S11.1). In the former case, the 1585 cm^{-1} band is displaced to 1561 cm^{-1}, in agreement with the formation of a radical cation quinoidal structure. Noticeably, this band is displaced to lower frequencies relative to [10CPP]$^{\bullet+}$, as a sign of the attainment of a larger quinoidization in the shorter phenylene core. No appreciable spectral changes were observed in the experiment of C_{60} under pressure with [11]CPP, which is probably due to a lack of size matching.

In summary, we have performed a thorough study of the Raman properties of [*n*]cycloparaphenylenes, which can be considered as the first molecularly well-defined models of SWCNTs. We provide with some spectroscopic–structural relationships between: 1) the parallel behavior and dependence of the pseudo-RBMs in [*n*]CPPs with those RBM of

(*n*,*n*) armchair SWCNTs; 2) the ring cyclic strain, molecular-level benzene quinoidization and ring size; and 3) the transformation of "pure" cyclic π-electron conjugation into pseudo-linear conjugation (cyclically embedded). On the other hand, high-pressure studies allow: 1) new insights on the plastic and conformational properties of these nanohoop-shaped systems; and 2) proposal of the formation of a charge transfer complex, $[10]CPP^{\bullet+}@C_{60}^{\bullet-}$, as a further progress relative to the already-known π–π van der Waals $[10]CPP@C_{60}$ supramolecular analogue. Overall, our study is a complete initiative to correlate structural, spectroscopic, and chemical properties in well-defined [*n*]CPP models and to relate such properties with those of SWCNTs.

Received: January 22, 2014
Revised: March 18, 2014
Published online: May 18, 2014

Keywords: charge-transfer salts · cycloparaphenylenes · pressure-dependent studies · Raman spectroscopy · single-wall carbon nanotubes

[1] M. J. O'Connell, *Carbon Nanotubes*: *Properties and Applications*, Taylor&Francis, Boca Raton, **2006**; P. J. F. Harris, *Carbon Nanotube Science*: *Synthesis Properties and Applications*, Cambridge University Press, Cambridge, **2009**.

[2] a) *Carbon nanotubes and Related structures*, *Synthesis Characterization*, *Functionalization and Properties* (Eds.: N. Martín, D. M. Guldi), Wiley-VCH, Weinheim, **2010**; b) R. Saito, G. Dresselhaus, M. S. Dresselhaus, *Physical Properties of Carbon Nanotubes*, Imperial College Press, London, **1998**.

[3] R. Jasti, J. Bhattacharjee, J. B. Neaton, C. R. Bertozzi, *J. Am. Chem. Soc.* **2008**, *130*, 17646 – 17647.

[4] J. Xia, R. Jasti, *Angew. Chem.* **2012**, *124*, 2524 – 2526; *Angew. Chem. Int. Ed.* **2012**, *51*, 2474 – 2476; T. J. Sisto, M. R. Golder, E. S. Hirst, R. Jasti, *J. Am. Chem. Soc.* **2011**, *133*, 15800 – 15802; T. J. Sisto, R. Jasti, *Synlett* **2012**, *23*, 483 – 489; E. S. Hirst, R. Jasti, *J. Org. Chem.* **2012**, *77*, 10473 – 10478; R. Jasti, C. R. Bertozzi, *Chem. Phys. Lett.* **2010**, *494*, 1 – 7; J. Xia, J. W. Bacon, R. Jasti, *Chem. Sci.* **2012**, *3*, 3018 – 3021.

[5] M. R. Golder, B. M. Wong, R. Jasti, *Chem. Sci.* **2013**, *4*, 4285 – 4291; E. Kayahara, T. Kouyama, T. Kato, H. Takaya, N. Yasuda, S. Yamago, *Angew. Chem.* **2013**, *125*, 13967 – 13971; *Angew. Chem. Int. Ed.* **2013**, *52*, 13722 – 13726; A. V. Zabula, A. S. Filatov, J. Xia, R. Jasti, M. A. Petrukhina, *Angew. Chem.* **2013**, *125*, 5137 – 5140; *Angew. Chem. Int. Ed.* **2013**, *52*, 5033 – 5036.

[6] T. Iwamoto, Y. Watanabe, Y. Sakamoto, T. Suzuki, S. Yamago, *J. Am. Chem. Soc.* **2011**, *133*, 8354 – 8365; S. Yamago, Y. Watanabe, T. Iwamoto, *Angew. Chem.* **2010**, *122*, 769 – 771; *Angew. Chem. Int. Ed.* **2010**, *49*, 757 – 759; E. Kayahara, Y. Sakamoto, T. Suzuki, S. Yamago, *Org. Lett.* **2012**, *14*, 3284 – 3287.

[7] T. Iwamoto, Y. Watanabe, T. Sadahiro, T. Haino, S. Yamago, *Angew. Chem.* **2011**, *123*, 8492 – 8494; *Angew. Chem. Int. Ed.* **2011**, *50*, 8342 – 8344.

[8] H. Omachi, S. Matsuura, Y. Segawa, K. Itami, *Angew. Chem.* **2010**, *122*, 10400 – 10403; *Angew. Chem. Int. Ed.* **2010**, *49*, 10202 – 10205.

[9] H. Takaba, H. Omachi, Y. Yamamoto, J. Bouffard, K. Itami, *Angew. Chem.* **2009**, *121*, 6228 – 6232; *Angew. Chem. Int. Ed.* **2009**, *48*, 6112 – 6116; Y. Segawa, S. Miyamoto, H. Omachi, S. Matsuura, P. Senel, T. Sasamori, N. Tokitoh, K. Itami, *Angew. Chem.* **2011**, *123*, 3302 – 3306; *Angew. Chem. Int. Ed.* **2011**, *50*, 3244 – 3248; H. Omachi, Y. Segawa, K. Itami, *Acc. Chem. Res.* **2012**, *45*, 1378 – 1389; Y. Ishii, Y. Nakanishi, H. Omachi, S. Matsuura, K. Matsui, H. Shinohara, Y. Segawa, K. Itami, *Chem. Sci.* **2012**, *3*, 2340 – 2345.

[10] H. Omachi, T. Nakayama, E. Takahashi, Y. Segawa, K. Itami, *Nat. Chem.* **2013**, *5*, 572 – 576.

[11] Y. Segawa, A. Fukazawa, S. Matsuura, H. Omachi, S. Yamaguchi, S. Irle, K. Itami, *Org. Biomol. Chem.* **2012**, *10*, 5979 – 5984; C. Camacho, T. A. Niehaus, K. Itami, S. Irle, *Chem. Sci.* **2013**, *4*, 187 – 195; T. Nishihara, Y. Segawa, K. Itami, Y. Kanemitsu, *J. Phys. Chem. Lett.* **2012**, *3*, 3125 – 3128.

[12] U. H. F. Bunz, S. Menning, N. Martín, *Angew. Chem.* **2012**, *124*, 7202 – 7209; *Angew. Chem. Int. Ed.* **2012**, *51*, 7094 – 7101; S. Schrettl, H. Frauenrath, *Angew. Chem.* **2012**, *124*, 6673 – 6675; *Angew. Chem. Int. Ed.* **2012**, *51*, 6569 – 6571.

[13] M. S. Dresselhaus, A. Jorio, R. Saito, *Annu. Rev. Condens. Matter Phys.* **2010**, *1*, 89 – 108.

[14] "Light Scattering in Solid IX": C. Thomsem, S. Reich, *Top. Appl. Phys.* **2007**, *108*, 115 – 232.

[15] Y. Segawa, H. Omachi, K. Itami, *Org. Lett.* **2010**, *12*, 2262 – 2265.

[16] E. H. Hároz, J. G. Duque, X. Tu, M. Zheng, A. R. H. Walker, R. H. Hauge, S. K. Doorn, J. Kono, *Nanoscale* **2013**, *5*, 1411 – 1435.

[17] A. Jorio, A. G. S. Filho, G. Dresselhaus, M. S. Dresselhaus, A. K. Swan, M. S. Ünlü, B. B. Goldberg, M. A. Pimenta, J. H. Hafner, C. M. Lieber, R. Saito, *Phys. Rev. B* **2002**, *65*, 155412.

[18] L. Cuff, C. Cui, M. Kertesz, *J. Am. Chem. Soc.* **1994**, *116*, 9269 – 9274; J. Casado, S. Patchkovskii, M. Z. Zgierski, L. Hermosilla, C. Sieiro, M. M. Oliva, J. T. López Navarrete, *Angew. Chem.* **2008**, *120*, 1465 – 1468; *Angew. Chem. Int. Ed.* **2008**, *47*, 1443 – 1446; S. R. González, Y. Ie, Y. Aso, J.-T. López Navarrete, J. Casado, *J. Am. Chem. Soc.* **2011**, *133*, 16350 – 16353.

[19] G. Heimel, D. Somitsch, P. Knoll, J. L. Brédas, E. Zojer, *J. Chem. Phys.* **2005**, *122*, 114511.

[20] A. San-Miguel, *Chem. Soc. Rev.* **2006**, *35*, 876 – 889.

[21] V. G. Baonza, M. Taravillo, A. Arencibia, M. Cáceres, J. Núñez, *J. Raman Spectrosc.* **2003**, *34*, 264 – 270.

[22] Z. S. Zhao, X. F. Zhou, M. Hu, D. L. Yu, J. L. He, H.-T. Wang, Y. J. Tian, B. Xu, *J. Superhard Mater.* **2012**, *34*, 371 – 385.

[23] M. Yao, Z. Wang, B. Liu, Y. Zou, S. Yu, W. Lin, Y. Hou, S. Pan, M. Jin, B. Zou, T. Cui, G. Zou, B. Sundqvist, *Phys. Rev. B* **2008**, *78*, 205411.

[24] a) E. del Corro, J. González, M. Taravillo, E. Flahaut, V. G. Baonza, *Nano Lett.* **2008**, *8*, 2215 – 2218; b) A. L. Aguiar, E. B. Barros, R. B. Capaz, A. G. S. Filho, P. T. C. Freire, J. M. Filho, D. Machon, C. Caillier, Y. A. Kim, H. Muramatsu, M. Endo, A. San-Miguel, *J. Phys. Chem. C* **2011**, *115*, 5378 – 5384.

[25] B. Anis, F. Börrnert, M. H. Rümmeli, C. A. Kuntscher, *J. Phys. Chem. C* **2013**, *117*, 21995 – 22001.

[26] B. W. Smith, M. Monthioux, D. E. Luzzi, *Nature* **1998**, *396*, 323 – 324.

[27] M. S. Dresselhaus, G. Dresselhaus, P. C. Eklund, *J. Raman Spectrosc.* **1996**, *27*, 351 – 371.

